# Wind Excitation and Severity of Standards Used for the Vibration Testing of Luminaires

F. Marin[1], J.-C. Golinval[1], C. Marville[2], A. Blochouse[2]
[1]Université de Liège, Département d'Aérospatiale, Mécanique et Matériaux
Vibrations & Identification des Structures
Chemin des chevreuils 1 (B52), 4000 Liège
[2]R-TECH
Schréder Group GIE
Rue de Mons 3, 4000 Liège
email: F.Marin@ulg.ac.be, JC.Golinval@ulg.ac.be, Christian.Marville@rtech.be, Arlette.Blochouse@rtech.be

*Abstract*— **During their lifetime, street lighting devices (or luminaires) are subject to environmental excitations induced by the traffic and the wind. Fatigue effects due to ambient vibrations of long duration are the main cause of structural failures in outdoor pole mounted luminaires. Street lighting manufacturers are very much concerned with vibration testing of luminaire prototypes in order to determine if they can support the vibration environment expected during their lifetime without being damaged. Up to now, qualification tests are performed according to different standards which are not specific to street lighting devices. These standards do not have the same severity so that the choice of one standard rather than another is not obvious. The aim of the research presented here is to propose a new methodology to quantify the severity of different vibration environments. To this end, different severity criteria are first defined. Based on these criteria, the severity of wind excitation and standards such as IEC 68-2-6 and ANSI C 136-31 may be estimated and compared.**

*Keywords*— **luminaire, shaker, accelerated fatigue testing, vibration environment severity, wind excitation**

## I. Introduction

The objective of the paper is to present a methodology to quantify the severity of vibration environments. The first step consists in reviewing the possible standards used for the vibration testing of luminaires such as the International Electrotechnical Commission IEC 68-2-6 and the American National Standard for Roadway Lighting ANSI C 136-31. The second step introduces the methodology to compute the spectral response of the pole–luminaire system to random excitations taking into account the effects of turbulent wind and Von Karman vortices [1]. The wind model is built on recent data of the Royal Meteorological Institute of Belgium. The third step deals with the definition of severity criteria built on a base excited one degree of freedom reference system : maximax response spectrum, fatigue damage spectrum or dissipative damage spectrum. To choose the most appropriate criterion, the identification and the knowledge of failure processes are of prime importance. The generalisation of fatigue damage spectrum computation to multi-degree-of-freedom systems is also presented. The methodology uses the stress time response provided by a finite element model to compute damage using a cycle counting method (*Rainflow*). An accelerated fatigue testing methodology, based on an optimisation process, minimises the difference between the severity of the wind vibration environment and the severity of the equivalent test to be performed in laboratory [1]. Finally, the methodology is validated on the example of a clamped beam submitted to vibration testing on an electro-dynamic shaker. Stress measurements are obtained by means of strain gauges and the damage is also computed using the rainflow method.

## II. Vibration Testing of Luminaires

### *A. The International Electrotechnical Commission IEC 68-2-6 Standard*

This standard describes a testing method applicable to components, equipment and other articles which, during transportation or in service, may be subjected to conditions involving vibration of a harmonic pattern, generated primarily by rotating, pulsating or oscillating forces, such as occur in ships, aircraft, land vehicles, rotorcraft and space applications or are caused by machinery and seismic phenomena [2]. It consists basically of submitting a specimen to sinusoidal vibration over a given frequency range or at discrete frequencies for a given period of time. The object of the standard is to provide a standard procedure to determine the ability of components, equipment and other articles to withstand specified severities of sinusoidal vibration. It is emphasised that vibration testing always demands a certain degree of engineering judgement, and both the supplier and purchaser should be fully aware of this fact. The main part of this standard deals primarily with the methods of controlling the test at specified points, and gives, in detail, the testing procedure. The requirements for the vibration motion, choice of severities including frequency ranges, amplitudes and endurance times are also specified; these severities representing a rationalised series of parameters. The relevant specification writer is expected to choose the testing procedure and values appropriate to the specimen and its use. Today, one can find some data and indications in previous proposals.

Some 26 years ago, introduction of vibration tests in the IEC 60598 standard [3] (Luminaires - General requirements and tests) has been discussed by IEC Experts Working Group LUMEX. This resulted in a project with two options : a first procedure aligning with IEC 68-2-6, reproducible and therefore suitable for possible introduction in a standard and a second procedure making use of a specific testing equipment like a shaking machine, simple but less reproducible than the first procedure. At the Brussels meeting (1977) of IEC-Technical Committee N. 34 (lamps and related equipment)-Sub-committee 34D (luminaires),

it was decided to keep the proposal at the Secretariat stage for information only. In the above options, the first proposal suggested that :
- in view of the difficulties of rigorously defining resonance, an endurance test should be made by sweeping over a sinusoidal frequency range (a random vibration test is considered unnecessarily sophisticated for the luminaires covered by the specification);
- definitions and values for the various parameters should be taken from IEC Publication 68-2-6;
- short and rigid mounting piece should be used such that no resonance of this mounting piece (without luminaire) should occur within 150 % of the maximum test frequency;
- the control point should be as close as possible to the fixing point;
- the sweep rate should be one octave per minute;
- the test should be performed along each structural axis.

In 1998, the introduction of a specific vibration test for rough service luminaires in the IEC standard 60598 was voted by the International Electrotechnical Commission. It means specific requirements for luminaires used in rough environment situations such as engineering workshops, building sites and similar applications. The vibration requirements are :
- a test is made by sweeping over the sinusoidal frequency range [10-55-10] Hz;
- the imposed displacement must be constant and equal to 0.35 mm;
- the duration of the endurance test is 30 minutes;
- the sweep rate is one octave per minute;
- the test must be performed along the most onerous direction.

Taking into account the different remarks mentioned in this paragraph, an example of test following IEC 68-2-6 requirements is given in table I.

TABLE I
POSSIBLE STANDARDS AND PARAMETERS FOR THE VIBRATION TESTING OF LUMINAIRES.

| **Standard** | **IEC 68-2-6** | **ANSI C 136-31** |
|---|---|---|
| **Excitation** | sine sweep | sine |
| | [10-55-10] Hz | $f_0 \in$ [5-30] Hz |
| **Amplitude** | 0.15 mm | 1.5 (3) g |
| | fixing point | centre of gravity |
| **Duration** | 100 sweeps | 100 000 cycles |

### *B. The American National Standard for Roadway Lighting ANSI C 136-31 Standard*

The USA ANSI C 136-31 new standard (2001) proposes that a requirement for a minimum vibration withstand capability be considered for luminaires for road and street lighting. According to the proposal, there are factors that may cause externally induced vibration effects but which may not be adequately covered by the application of a static load test. For this reason, a vibration test might serve as a more appropriate and suitable substitute. This ANSI Standard will probably be included in the new CANENA Luminaire Standard that will harmonise Canadian, U.S. and Mexican requirements. This new standard suggests that :
- the fundamental resonant frequency must be determined for each of the three perpendicular planes and must be between 5 and 30 Hz;
- the luminaire must be vibrated at or near his natural frequency;
- the acceleration intensity measured at the luminaire centre of gravity must be 1.5 g for normal roadway applications and 3 g for bridge and overpass applications;
- the lighting device must be capable of withstanding the described vibration for 100 000 cycles in each plane.

Table I summarises the standards used for the vibration testing of luminaires.

## III. EXCITATION OF STREET–LIGHTING STRUCTURES

In order to have a better knowledge of the luminaire vibration environment, the dynamic response of the pole–luminaire system subject to random aerodynamic excitations (traffic effect is not taken into account) can be computed. The mathematical model used for the simulation is linear and based on the finite element method [4]. The assumptions related to the modelling are the following :
- the pole behaves as a beam;
- the luminaire is considered as a rigid body and is modelled by a concentrated mass at its center of gravity.

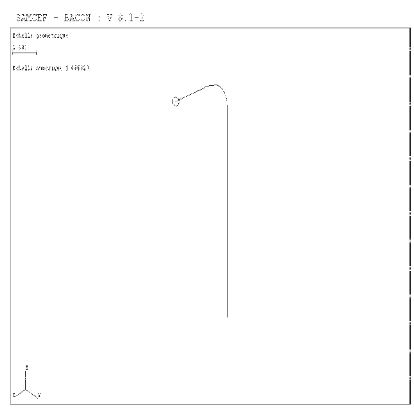

Fig. 1. Finite element model in structural axes.

The pole–luminaire system is described as shown in figure 1, where the linear vibrations of the structure are governed by the differential equation system (1).

$$\mathbf{M}\,\ddot{\mathbf{x}} + \mathbf{C}\,\dot{\mathbf{x}} + \mathbf{K}\,\mathbf{x} = \mathbf{f} \tag{1}$$

$\mathbf{M}$, $\mathbf{C}$ and $\mathbf{K}$ are respectively the mass, damping and stiffness matrices. The last one is the sum of the structural and geometric stiffness matrices [4]. The vectors $\mathbf{x}$ and $\mathbf{f}$ represent, in structural axes, the displacement and force acting on each degree of freedom of the finite element model.

Once the independant random aerodynamic excitations are known (turbulent wind and Von-Karman vortices), the supposed elastic linear behaviour of the structure easily allow to solve separately the problems in the frequency domain [5]. If $r$ is a response quantity (e.g. a stress component or a displacement) linearly related to the modal amplitudes $\mathbf{y}$ of a structure exposed to a field of random forces, its *Power Spectral Density (PSD)* function can be computed according to the following steps (figure 2) :

- compute the modal excitation *PSD* matrix $\mathbf{\Phi_P}(\omega)$ from the excitation *PSD* matrix $\mathbf{\Phi_F}(\omega)$ and the mode shape matrix $\mathbf{\Xi}$;
- compute the modal response *PSD* matrix $\mathbf{\Phi_y}(\omega)$ from the excitation *PSD* matrix $\mathbf{\Phi_F}(\omega)$ and the modal transfer matrix $\mathbf{H}(\omega)$;
- compute the response *PSD* function $\Phi_r(\omega)$.

As one can see, the procedure is computationally simple as soon as the damping data, transfer matrix are available and the excitation has been defined. This latter point turns out to be the most difficult one for most physical problems.

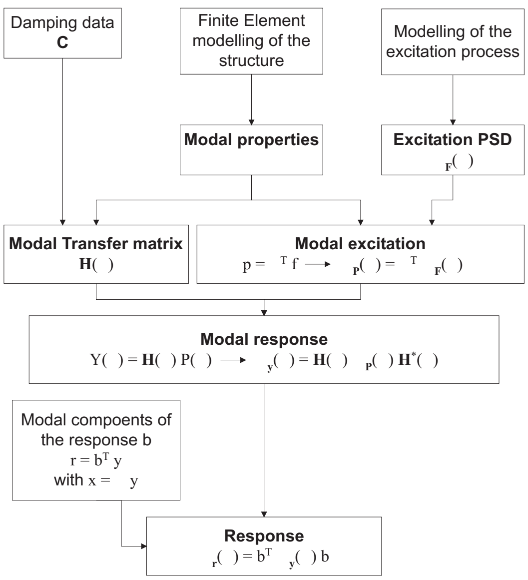


Fig. 2. Spectral analysis.

## A. Effect of Turbulent Wind

Near the ground, a boundary layer is mainly generated by the friction forces. The analysis of the wind frequency distribution reveals that an important part of the energy is concentrated on a period of time of one minute which corresponds to turbulent movements. If one defines wind relative axes, represented in structural axes by the azimuth ($\alpha_1$) and elevation ($\alpha_2$) angles, the instantaneous speed at time t for a point p of the space may be represented by the sum of the mean wind velocity and of a stochastic process which represents the along wind speed fluctuations around its mean value.

$$V(p,t) = u(p) + u'(p,t) \qquad (2)$$

If the mean wind speed is fixed, one obtains a short term model of the instantaneous speed which accounts for the fluctuations due to the atmospheric turbulence. This process considered as stationary on a period of time T, of about ten minutes, is defined by its *Power Spectral Density* matrix [5]. The turbulent wind model used in this study is based on *Davenport*'s spectrum [6].

$$\Phi_{\xi_i \xi_j}(\omega) = \frac{4\,\kappa\, u_{10}^2}{u_i\, u_j\, \omega}\, \frac{(\frac{600\,\omega}{\pi\, u_{10}})^2}{[1+(\frac{600\,\omega}{\pi\, u_{10}})^2]^{4/3}}\, \exp(-\frac{\omega}{2\,\pi\, u_{10}}\, C_z\, |z_i - z_j|) \quad (3)$$

with $0 < \omega < +\infty$ and $\xi_i = u'_i/u_i$. Equation (3) depends on the roughness of the ground ($\kappa$), the reference meteorological speed ($u_{10}$) measured at 10 m above the ground, the wind mean velocity ($u_i$) depending on the altitude of point i [5], the pulsation ($\omega$) and a term of spatial coherence function of the vertical correlation constant ($C_z$) and of the distance between two points i and j along the vertical axis. When a structure is subject to wind effect, aerodynamic forces are generated. In this approach, only the effect of the wind speed turbulent component is considered (the static component does not produce vibrations). If one assumes that

- the structure does not modify the incident turbulent flow;
- the aerodynamic coefficients of the structure are measured in the stationary flow $u(p)$;
- $O(u'^{\,2}) \ll O(u^2)$;

the wind instantaneous velocity can be linearised and the *PSD* matrix of forces $\mathbf{\Phi_{C_iC_j}}(\omega)$ is obtained from equation (3) by introducing the profile aerodynamic properties $\boldsymbol{\nu}_\mathbf{i}$ [5], [7] :

$$\mathbf{\Phi_{C_iC_j}}(\omega) = \boldsymbol{\nu}_\mathbf{i}\, \boldsymbol{\nu}_\mathbf{j}^\mathbf{T}\, \mathbf{\Phi}_{\boldsymbol{\xi}_\mathbf{i}\boldsymbol{\xi}_\mathbf{j}}(\omega) \qquad (4)$$

$$\begin{cases} \boldsymbol{\nu}_\mathbf{i} = \rho\, u_i^2\, (S_i\, \mathbf{C_{F_i}})_{(\alpha_1,\alpha_2)} & \text{force coefficient} \\ \boldsymbol{\nu}_\mathbf{i} = \rho\, u_i^2\, (V_i\, \mathbf{C_{T_i}})_{(\alpha_1,\alpha_2)} & \text{torque coefficient} \end{cases}$$

where $\rho$ is the air density, $S_i$ and $V_i$ are the area and volume associated with point i, $\mathbf{C_{F_i}}$ and $\mathbf{C_{T_i}}$ are the aerodynamic force and torque coefficients at i.

## B. Effect of Von–Karman Vortices

A second type of excitation induced by the wind is the action of the wake on the structure. For a particular rate of flow, characterised by its *Reynolds* number ($R_e$), vortices are shed in the wake inducing across–wind vibrations on the pole–luminaire system. While fluctuating forces due to wind turbulence seem to be predictable with reasonable accuracy and simplicity, the understanding of the physical mechanism of wake excitation has proved to be much more complex and the application of analytical methods to predict the related wind loading is still fairly uncertain. The theory first developed by *Vickery* simulated Von–Karman vortices by a *PSD* of a Gaussian function $\Phi_{f_i f_j}(\omega)$ [8]. In order to improve the accuracy of function $f_i$ in the low and high frequency ranges, the function used in this study is taken from reference [9] :

$$f_i = \frac{\frac{\beta_i\,(1-0.64\,\beta_i^2)\,\omega}{(0.964-0.353\,\beta_i)\,\omega_{si}^2}}{\left[1-\left(1-0.64\,\beta_i^2\right)\,\frac{\omega^2}{\omega_{si}^2}\right]^2 + 2.56\,\beta_i^2\,\left(1-0.64\,\beta_i^2\right)\,\frac{\omega^2}{\omega_{si}^2}} \qquad (5)$$

where $\beta_i$ is a bandwidth parameter function of longitudinal turbulence intensity and $\omega_{si}$ is the shedding frequency at height $z_i$ [9]. Finally, the across–wind *PSD* matrix of forces $\mathbf{\Phi_{F_iF_j}}(\omega)$ is obtained by introducing the profile aerodynamic properties $\boldsymbol{\nu}_\mathbf{i}^\mathbf{vk}$ [9] :

$$\mathbf{\Phi_{F_iF_j}}(\omega) = \boldsymbol{\nu}_\mathbf{i}^\mathbf{vk}\, \boldsymbol{\nu}_\mathbf{j}^\mathbf{vkT}\, \mathbf{\Phi_{f_if_j}}(\omega) \qquad (6)$$

$$\begin{cases} \boldsymbol{\nu}_\mathbf{i}^\mathbf{vk} = \frac{1}{2}\,\rho\, u_{ni}^2\, (\tilde{S}_i\, \mathbf{\tilde{C}_{F_i}})_{(\alpha_1,\alpha_2)} & \text{force coefficient} \\ \boldsymbol{\nu}_\mathbf{i}^\mathbf{vk} = \frac{1}{2}\,\rho\, u_{ni}^2\, (\tilde{V}_i\, \mathbf{\tilde{C}_{T_i}})_{(\alpha_1,\alpha_2)} & \text{torque coefficient} \end{cases}$$

where $u_{ni}$ is the mean wind velocity normal to the structure at i, $\tilde{S}_i$ and $\tilde{V}_i$ are the area and volume associated with point i, $\tilde{\mathbf{C}}_{\mathbf{F_i}}$ and $\tilde{\mathbf{C}}_{\mathbf{T_i}}$ are the aerodynamic force and torque coefficients at i for Von–Karman vortices.

### *C. Application to Recent Data of the Royal Meteorological Institute of Belgium*

The wind model is built on recent data of the Royal Meteorological Institute of Belgium. Two different wind intensities are considered :

- a mean wind, characterised by a reference meteorological speed $u_{10}$=10.2 m/s (estimated during the period 1985-1996) and a duration equal to the lifetime of the luminaire i.e., 20 years;
- a severe wind, characterised by a reference meteorological speed $u_{10}$=19.6 m/s (estimated during the storm of October 2002 in Belgium), a duration of 9 hours and a return probability of 2 years.

The methodology has been applied to a common pole–luminaire system like the one shown in figure (1). The response is computed at the fixing point of the luminaire on the pole for different wind orientations. In order to obtain the more severe excitation, the envelop of all the responses computed following the three structural axes is taken into account. The parameter of the model are the following : site roughness II, damping ratio $\varepsilon$ = 0.5 %, luminaire mass 10 kg and pole height 10 m. Figure (3) represents the envelop of the response *PSD* for the two considered meteorological speeds.

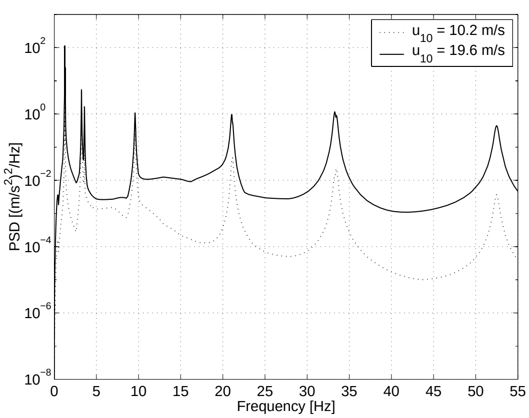


Fig. 3. Response of the pole–luminaire system.

## IV. Severity of Vibration Environments

Once the excitation is known (standard parameters or reponse of the pole–luminaire system), it can be used to compute the severity of the luminaire vibration environment.

Three basic criteria are available in the literature [10], [11] to quantify the severity of vibration environments :

- the maximax response spectrum, associated with the maximum displacement representative of the maximum stress in the equipment;
- the fatigue damage spectrum, which is related to the deterioration of the material when submitted to repeated stresses;
- the dissipative damage spectrum, based on the assumption that the energy dissipated by the equipment is correlated with the severity of the vibration environment.

Since fatigue effects of long time ambient vibration are the leading cause of structural failures in outdoor pole mounted luminaires, the most representative criterion is the *fatigue damage spectrum.* In the frequency range of interest [10-55] Hz, measurement results show that only the first mode shape of the luminaire is generally excited. For this reason, the definition of severity criteria is based on the application of the vibration excitation to the base of a reference one-degree-of-freedom system (figure 4). The generalisation of fatigue damage spectrum computation to multi-degree-of-freedom systems is also presented.

### *A. Reference One–degree–of–freedom System*

The equation of movement of such a system is given by the relation (7)

$$\ddot{z} + 2\,\varepsilon\,\omega_0\,\dot{z} + \omega_0^2\,z = -\ddot{x} \tag{7}$$

where $x(t)$ describes the motion imposed to the base, $z(t)$ the relative position of the mass, $\varepsilon$ the damping ratio and $\omega_0$ the natural pulsation of the one–dof system. The mass $m$, stiffness $k$ and damping $c$ are the parameters of a modal model of the luminaire obtained either by finite element analysis or by experimental modal identification.

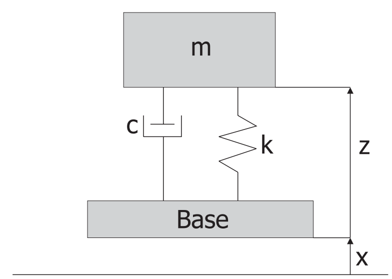


Fig. 4. Reference 1–dof mass–spring–damper system.

For a given vibration environment $x(t)$, the maximal response $Z_{max}$ of the relative displacement is a function of the natural frequency $f_0$ and of the damping ratio $\varepsilon$. For a stress level $\sigma_i$, the corresponding damage $d_i$ is defined by $d_i = n_i/N_i$, $n_i$ being the number of cycles of amplitude $\sigma_i$ and $N_i$ the maximum number of cycles before deterioration at the same stress level. $N_i$ is given by the classical Wöhler curves of the material, which in their central part, can be approximated by *Basquin*'s relationship :

$$N_i\,\sigma_{i,max}^b = A^b \tag{8}$$

where $b$ and $A$ are two material dependent parameters. If one assumes a linear behaviour of the material, stress and displacement may be related by a constant $K$ :

$$\sigma_{i,max} = K\,Z_{i,max} \tag{9}$$

According to *Miner*'s linear cumulative damage law and using equations (8–9), one obtains the total damage $D$ corresponding to the reference 1–dof system in the form :

$$D = \left(\frac{K}{A}\right)^b \sum_i n_i\,Z_{i,max}^b\,(f_0, \varepsilon) \tag{10}$$

The fatigue damage spectrum is the curve which represents the total damage $D$ as a function of the natural frequency $f_0$, for a given $\varepsilon$. Consequently, the comparison between two vibration environment will be centred on the assumption that two environments have the same severity if they induce the same damage to the reference 1-dof system. In the cases of a sinusoidal excitation at discrete frequency (ANSI C 136-31 standard), a logarithmic sine sweep excitation (IEC 68-2-6 standard) or a random Gaussian excitation (wind effect), the expected value of $Z_{i,max}$ may be calculated by the theory of harmonic and random vibrations [5], [10], [11]. The localisation in the structure of the maximal stress needs the use of a more elaborate finite element model or of an experimental model with strain gauges.

### *B. Generalisation to Multi-degree-of-freedom Systems*

To localise the maximal stress in the structure, a more elaborated finite element model taking into account the geometry of the structure needs to be used. Figure 5 summarises the different steps constituting the general methodology for the computation of fatigue damage.

The starting point of the methodology is the finite element modelling of the structure. A dynamic analysis solves the following homogeneous equation system

$$\mathbf{M}\,\ddot{\mathbf{x}} + \mathbf{K}\,\mathbf{x} = 0 \tag{11}$$

providing the modal parameters : natural frequencies $f_0$ and mode shapes $\Xi$. A comparison of the computed modal parameters with the ones identified by an experimental modal analysis allows to verify the quality of the modelling and to update it if necessary. The experimental modal analysis is also necessary to estimate the modal damping ratios. The linear vibrations of a base excited structure subject to a sinusoidal, sine sweep or random excitation are governed by the differential equation system given by equation (1) where f represents the structural forces acting on each degree of freedom of the interface. The supposed elastic linear behaviour of the structure easily allows to solve the problem in the frequency domain providing as response the maximal stress observed in one element during one cycle at the excitation frequency.

The last step of the finite element analysis consists in generating the stress time history from the results obtained in the frequency domain. In the case of sinusoidal or sine sweep excitations, the assumption is made that an harmonic excitation induces an harmonic response. The expression of the stress time history can be written as

$$\sigma(t) = Y_\sigma(\omega)\,\cos(\omega\,t) \tag{12}$$

In the case of random excitation, the stress time history is computed from the stress *Power Spectral Density* $\Phi_\sigma(\omega)$. The idea is to generate a sequence of *Discrete Fourier Transform* coefficients with amplitude and phase such that the *Inverse Discrete Fourier Transform* will produce the desired time sequence $\sigma(t)$. If we choose the phases as independent random variables with uniform distribution in [0-2$\pi$], for any time t, any new set of statistically independent random phases produces a new sample record with

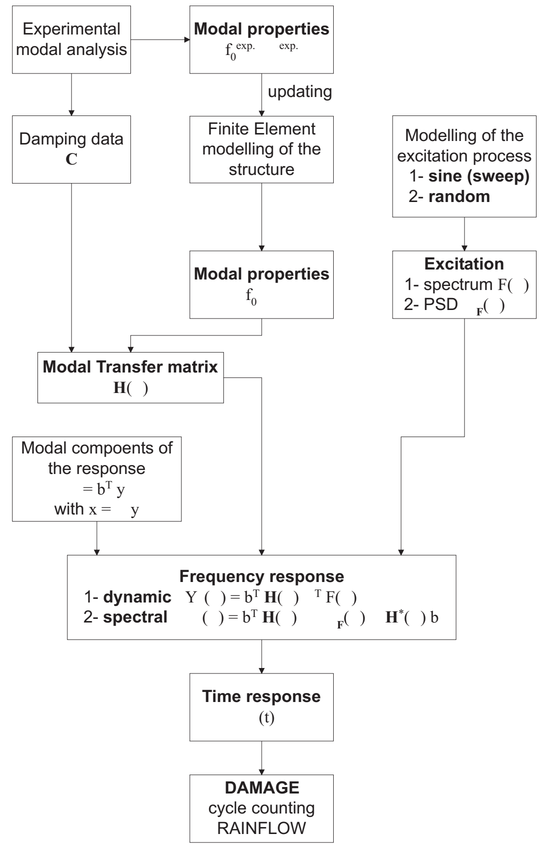


Fig. 5. General methodology for damage computation.

the same spectral content, but statistically independent of the previous record [5].

Once the stress time history is generated, the damage is computed by a cycle counting process based on the well-known *Rainflow* method [12], [13], [14]. The stress time history is decomposed into elementary cycles of known amplitude and average which are stocked in a *Rainflow* matrix R. The damage computation from the *Rainflow* matrix R is easily performed using *Basquin*'s relationship (8).

### *C. Accelerated Fatigue Testing Methodology*

To ensure a reliable design, fatigue vibration testing has to be carried out in laboratory in order to reproduce the real environment severity as accurately as possible. The objectives of the methodology are twofold :

- to define the vibration test specifications;
- to reduce the test duration.

The use of the severity criteria, developed for a 1–dof system and generalised to multi–degree–of–freedom system allows to compare the severity of two different vibration environments. For a vibration defined in a given frequency range $[f_1, f_2]$, the methodology, consists in :

1. computing the severity criterion for the reference vibration environment;
2. searching the equivalent test specifications so that the test duration is reduced and the equivalence from a severity point of view is obtained.

The research of the equivalent test can be performed using analytical expressions of criteria or using an iterative

process based on an optimisation process. The advantages of the last method are the following :
- there is no restriction on the value of the natural frequency $f_0$ which may belong or not to $[f_1, f_2]$;
- the method is efficient even for complex problems (complex excitations, multi–degree–of–freedom systems).

This methodology [1] has been developed in the *Boss/QUATTRO* software [15]. The successive tasks are organised as shown in the flowchart of figure (6) :

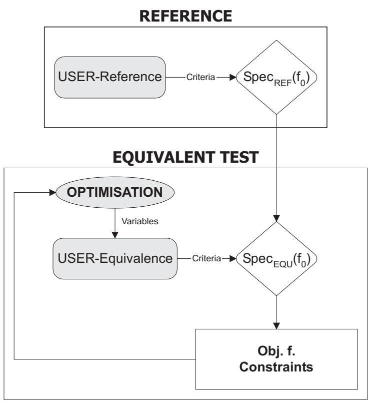


Fig. 6. Optimisation process in *Boss/QUATTRO*.

1. the script *USER-Reference* runs the computation of the comparison criterion for the reference test;
2. from the initial values of the design variables, the script *USER-Equivalence* computes the same criterion for the equivalent test;
3. using results obtained in steps 1 and 2, the objective function to minimise and the constraints are generated;
4. the sensitivities of the different functions with respect to each design variable are computed and the parameters up-dated;
5. steps 2 to 4 are repeated until an optimum is reached.

## V. Application Example

The developed methodology is illustrated on the simple case of a base excited beam supporting, as shown in figure (7), a concentrated mass at its free end (Ma=4.77 kg, r=0.04 m). The structure is made up of steel (A=886 MPa, b=7, $\sigma_u$=415 Mpa, $\sigma_e^0$=128 Mpa, Young modulus E=205 $10^3$ Mpa, density $\rho$=7850 kg/m3) and four different lengths are considered (L=0.575, 0.510, 0.475 and 0.445 m). The section of the beam is rectangular ($b_s$=0.08 m, $h_s$=0.015 m). Equation (9) has shown that the methodology based on the reference one-degree-of-freedom system requires the knowledge of the coefficient K relating the stress to the relative displacement. To this end, an analytical approach has been used to compute K. The general methodology centred on a finite element analysis is applied to a 3D volumic model of the beam. Vibration testing performed on an electro-dynamic shaker allows to validate the theoretical approaches. Stress measurements are obtained by means of strain gauges and the damage is computed using the *Rainflow* counting process.

The developed theory requiring a response computation has highlighted that both methodologies are subject to the same important unknown i.e., the damping ratio $\varepsilon$. In order to estimate this modal parameter, an experimental modal analysis has been first performed.

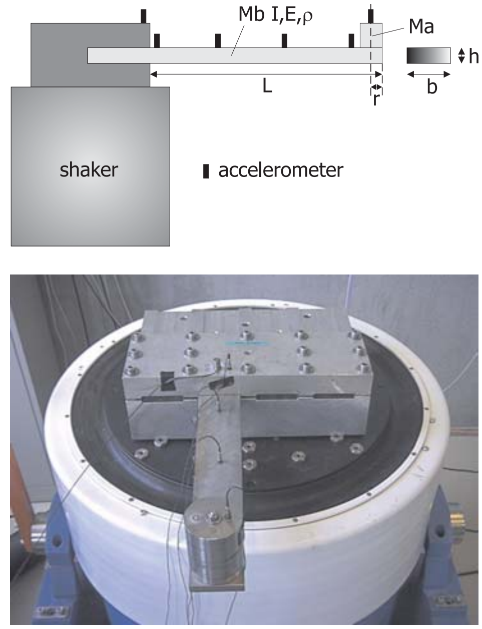


Fig. 7. Experimental test-case.

### A. Modal Parameter Identification

The modal parameters are identified using the *Frequency Response Functions (FRF)* measured during the different tests. The magnitude of such a function computed between the fixing point and the free end of the beam is shown in figure (8). It clearly appears that in the frequency range of interest [10-55] Hz, the behaviour of the structure may be approximated by a one-degree-of-freedom system (the peak represents the first bending mode shape of the beam).

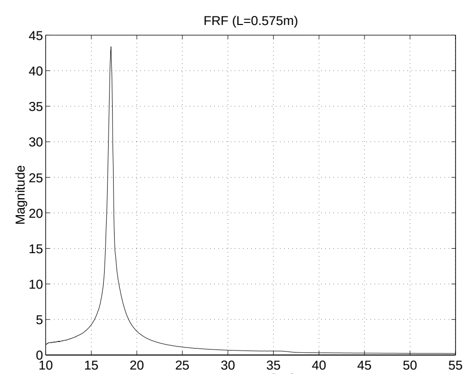


Fig. 8. FRF measured during the IEC 68-2-6 test.

Based on this assumption, the damping ratio is given by

$$Q = \frac{f_0}{\Delta f|_{\frac{|H|_{max}}{\sqrt{2}}}} \approx \frac{1}{2\,\varepsilon} \qquad (13)$$

and the results are summarised in table II. In the case of the wind excitation, a low level random excitation (0.5 $g_{RMS}$) has been performed in order to identify the modal parameters.

TABLE II
RESULTS OF THE MODAL PARAMETER ESTIMATION.

| | ANSI C 136-31 (roadway) | | IEC 68-2-6 | | Random (low level) | |
|---|---|---|---|---|---|---|
| $L[m]$ | $f_0$[Hz] | $\varepsilon$[%] | $f_0$[Hz] | $\varepsilon$[%] | $f_0$[Hz] | $\varepsilon$[%] |
| 0.575 | 17.1 | 0.37 | 16.9 | 1.24 | 16.6 | 0.81 |
| 0.510 | 20.2 | 0.79 | 20.0 | 1.40 | 19.7 | 1.04 |
| 0.475 | 22.5 | 0.69 | 21.9 | 2.29 | 22.1 | 1.38 |
| 0.445 | 24.8 | 1.26 | 24.1 | 3.42 | 23.6 | 1.92 |

The modal tests reveal that both the frequencies and damping ratios are subject to the amplitude level. Such a phenomenon is a characteristic of non-linear structures. The most plausible explanation is to admit that clamping is not perfect : its properties vary with the severity of the test. The identified damping ratios will nevertheless be used in the different damage computation methodologies.

### B. Reference One-degree-of-freedom System

As shown in reference [16], the analytical expression of coefficient K, in the particular case of a beam with a mass at its free end, can be written as

$$K = \frac{3Eh_s}{2L^2} \tag{14}$$

showing that for given material and section, K only depends on the length of the beam. For the four considered length of the beam, coefficient K is given in table III. The difference in natural frequencies between table II and table III is due to the simplifying assumptions of the analytical model :

- the mass Ma is concentrated at the end of the beam but it is not really true for the experimental test-case (r=0.04 m);
- perfect clamping is considered.

TABLE III
COEFFICIENT K FOR DIFFERENT LENGTHS OF THE BEAM.

| $L[m]$ | $f_0$[Hz] | $K[N/m^3]$ |
|---|---|---|
| 0.575 | 17.4 | 1.32 $10^{10}$ |
| 0.510 | 21.1 | 1.62 $10^{10}$ |
| 0.475 | 23.7 | 1.87 $10^{10}$ |
| 0.445 | 26.2 | 2.04 $10^{10}$ |

### C. General Methodology

The properties of the finite element model used for the damage computation are the following :

- the model is made up of 3D volumic shell elements;
- the mass Ma is concentrated at its centre of gravity;
- the clamping is modelled by spring elements;
- the model is updated on the first natural frequency.

Figure (9) shows the 3D volumic finite element model of the beam and the strain energy density map associated with the first bending mode shape. Such an iso-strain map highlights the critical areas (i.e., the clamping in the case of the present structure) where strain gauges should be placed to measure the maximal stress. For this reason, the finite element model is a precious aid to the positioning of strain gauges.

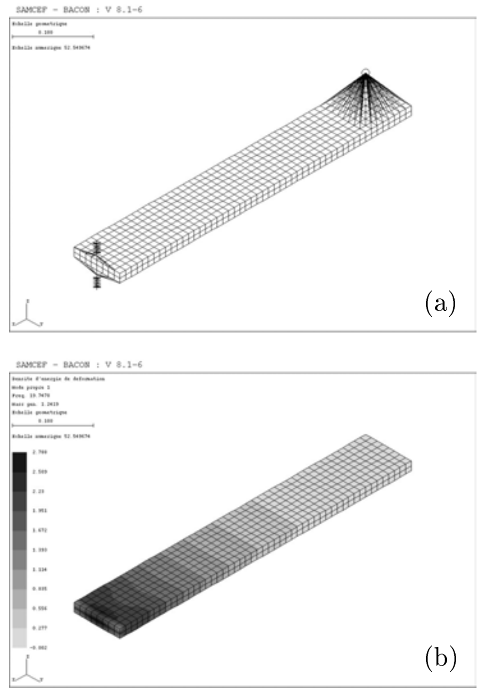


Fig. 9. (a) 3D volumic model - (b) Strain energy density of the $1^{st}$ mode shape.

### D. Results

The fatigue damage spectra resulting from the different computation methodologies and vibration environments applied to the base excited beam are compared in figure (10). The curves correspond to the reference one-degree-of-freedom system with the analytic computation of K. For a same excitation, each curve represents the fatigue damage spectrum for a given damping ratio constant in the frequency range [10-30] Hz. It appears that the severity of the wind excitation and IEC 68-2-6 standard is function of the damping ratio which is not the case with the ANSI C 136-31 standard for small damping ratio ($\varepsilon < 10$ %). In the last case, the excitation being performed at the centre of gravity of the structure, the ANSI C 136-31 standard will remain independent of the damping ratio until the base displacement may be considered small in comparison with the displacement at the centre of gravity. In the other cases, the shaker control being performed at the fixing point, the response at the centre of gravity is conditioned by the damping ratio. The circles, squares and triangles represent the results of computation and measurements for the four considered lenghts of the beam. The same remarks can be formulated about the effect of the damping ratio on standards severity. The comparison of measurement results with the computation results shows that the computation is conservative. The difference in stress belongs to the interval [4-20] %. Several sources of error can be pointed out [16] :

• the dependance of the computed reponse on the damping ratio;
• the effect of stress gradients in critical areas;
• the difficulty to perform in practice a sinusoidal excitation at natural frequency without the appropriate control system;
• the considered clamping model.

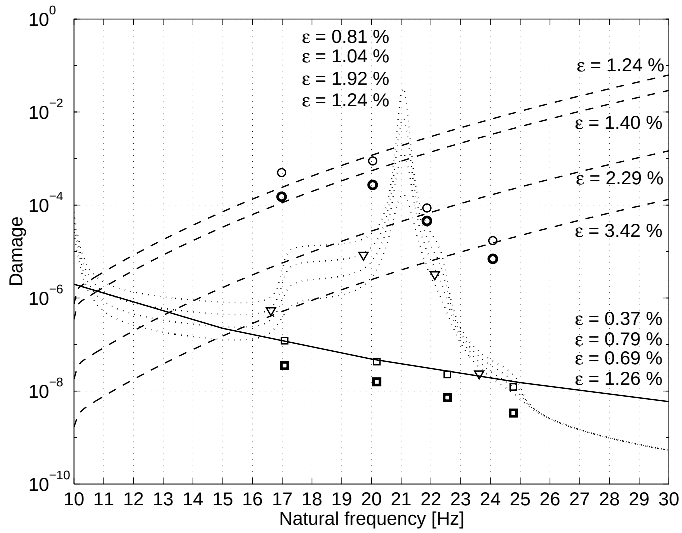


IEC 68-2-6 standard
**dashed lines** : 1dof/$K_{analytic}$ method
**black circles** : general method
**bold circles** : measurement results
ANSI C 136-31 standard (1.5 g)
**solid lines** : 1dof/$K_{analytic}$ method
**black squares** : general method
**bold squares** : measurement results
Wind excitation
**dotted lines** : 1dof/$K_{analytic}$ method
**black triangles** : general method

Fig. 10. Wind and standard severity comparison.

In the case of the wind induced vibrations, the generated damage is essentially due to the storm (factor ≈100). Figure (10) clearly shows that the severity of the test may significantly increase if one natural frequency of the luminaire coincides with one of the pole–luminaire system. The results of the spectral analysis have also been used as reference test in the presented accelerated fatigue testing methodology. The equivalent test corresponds to a random testing in the frequency range of [5-55] Hz. The allowable minimal frequency is imposed by the technical capabilities of electro–dynamic shakers. The test levels at 5 Hz and 55 Hz have been chosen as the design variables of the optimisation process for a duration of one hour. The specifications of the accelerated equivalent tests for the four lengths of the beam are summarised in table IV where $a_{RMS}$, $D$ and $\sigma^R_{max}$ are respectively the $RMS$ value of the excitation $PSD$, the damage and the quotient of the maximal stress observed in the equivalent and reference test. At the end of the optimisation process the relative difference between the reference and equivalent damage is equal to $10^{-3}$.

TABLE IV
Specifications of the equivalent tests.

| | **Amplitude** $[(m/s^2)^2/Hz]$ | | $\boldsymbol{a_{RMS}}$ $[m/s^2]$ | $\boldsymbol{D}$ [/] | $\boldsymbol{\sigma^R_{max}}$ [/] |
|---|---|---|---|---|---|
| $L[m]$ | 5[Hz] | 55[Hz] | | | |
| 0.575 | 5.1 $10^{-2}$ | 4.1 $10^{-2}$ | 2.3 | 5.4 $10^{-7}$ | 1.5 |
| 0.510 | 1.4 $10^{-1}$ | 1.4 $10^{-1}$ | 6.9 | 8.4 $10^{-6}$ | 1.9 |
| 0.475 | 1.5 $10^{-1}$ | 1.8 $10^{-1}$ | 8.4 | 3.2 $10^{-6}$ | 1.7 |
| 0.445 | 6.6 $10^{-2}$ | 5.5 $10^{-2}$ | 3.0 | 2.4 $10^{-8}$ | 1.7 |

## VI. Conclusions

The developed methodologies are based on the fatigue damage spectrum criterion. The choice of this criterion among others has been imposed by the identification and knowledge of failure processes. The ability to know and compare the severity of the standards used in the vibration testing of street lighting devices is of prime importance for the luminaire manufacturer.

Before being applied to a real luminaire, the different methods have been tested on the simple case of a base excited beam supporting a mass at its free end. The results obtained by measurement and computation have shown that the one-degree-of-freedom system methodology is a good approach to predict the damage spectrum behaviour of a structure subject, for example, to a sinusoidal excitation (damping ratio effect, excitation frequency effect). If a more accurate damage computation is needed, a more elaborate finite element model is to be taken into account. When the excitation is away from the natural frequency, a very good correlation between strain gauge measurements and model is obtained. Unfortunately, most of the time the first natural frequency of the device is included in the excitation frequency range imposed by standards. In this case, the effect of the damping ratio is of primary importance and the error on the stress prediction may be high. Other sources of error are the gauge positioning, the boundary conditions modelling, the difficulty to perform exactly a vibration test at the natural frequency, . . .

The simulation of the wind effects built on recent data of the Royal Meteorological Institute of Belgium has shown that the damage is essentially due to severe conditions like storms. The developed accelerated fatigue testing methodology has highlighted the possibility to obtain an equivalent test of reduced duration for a given pole–luminaire system.

## Acknowledgments

This research is funded by R-Tech (Schréder Group GIE) and the Walloon Region within the framework of the research convention 'First-Doctorat Entreprise n° 991/4177'. They are gratefully acknowledged.

## References

[1] F. Marin, J.-C. Golinval, C. Marville, *Accelerated Fatigue Testing Methodology of Luminaires on Electro-Dynamic Shaker*, Second International Conference on Advanced Computational Methods in Engineering, Liège (Belgium), May 28-31, 2002.
[2] International Standard IEC 68-2-6, *Environmental Testing - Part 2 : Tests - Test Fc : Vibration (sinusoidal)*, International Electrotechnical Commission, Sixth Edition, March 1995.

[3] International Standard IEC 60598-1, *Luminaires - General requirements and tests*, International Electrotechnical Commission, Fifth Edition, December 1999.

[4] M. Géradin, D. Rixen, *Mechanical Vibrations – Theory and Application to Structural Dynamics*, Masson, 1994.

[5] A. Preumont, *Random Vibration and Spectral Analysis*, Kluwer Academic Publishers, 1994.

[6] A.G. Davenport, *The application of statistical concepts to the wind loading of structures*, Proc. Inst. Civ. Eng., Vol. 19, 449–471, August 1961.

[7] S.F. Hœrner, *Résistance à l'avancement dans les fluides*, Gauthier–Villars Editeur, Paris, 1965.

[8] B.J. Vickery, A.W. Clark, *Lift or Across–Wind Response of Tapered Stacks*, Journal of the Structural Division, ASCE, Vol. 98 No. ST1, 1972.

[9] G. Solari, *Mathematical Model to Predict 3–D Wind Loading on Buildings*, Journal of Engineering Mechanics, Vol. 111 No. 2, 254–275, February 1985.

[10] F. Cambier, P. Dehombreux, O. Verlinden, C. Conti, *Equivalence criteria between mechanical environments*, European Journal of Mechanical Engineering, Vol. 41 No. 4, 219–226, 1997.

[11] Norme GAM–EG–13, *Essais généraux en environnement des matériels : annexe générale mécanique*, 1992.

[12] X. PITOISET, *Méthodes spectrales pour une analyse en fatigue des structures métalliques sous chargements aléatoires multiaxiaux*, Thèse de doctorat, Université Libre de Bruxelles, 2001

[13] N. E. DOWLING, *Mechanical Behavior of Materials*, Engineering Methods for Deformation, Fracture and Fatigue, Prentice Hall, Second Edition, 1999

[14] C. AMZALLAG, J.P. GEREY, J.L. ROBERT & J. BAHUAUD, *Standardization of the rainflow counting method for fatigue analysis*, International Journal of Fatigue, 16(4) : 287-293, 1994

[15] SAMTECH S.A., *Boss/QUATTRO v.2.1 User's Guide*, Liège.

[16] F. Marin, J.-C. Golinval, C. Marville, A. Blochouse, *Comparison of the Severity of Standards Used for the Vibration Testing of Luminaires*, Seventh International Testing Laboratories Exhibition (ASTELAB 2003), Paris, March 17-19, 2003.